Atomic Transition Probabilities of the Halogens*

Roger D. Bengtson,† Myron H. Miller, David W. Koopman, and T. D. Wilkerson
Institute for Fluid Dynamics and Applied Mathematics, University of Maryland, College Park, Maryland 20742
(Received 17 August 1970)

Absolute transition probabilities in the visible and near-infrared spectra of F I, Cl I, Cl II, and Br I have been measured using a gas-driven shock tube. Thermodynamic conditions in the source were overdetermined by line intensity, pressure, and electron-density data. *A* values were obtained by spectroscopic techniques which reduced errors due to residual uncertainties in the source conditions. Measured transition probabilities are compared with theoretical calculations and with other experimental values.

I. INTRODUCTION

Accurate measurements of absolute transition probabilities have usually concentrated upon a single spectrum or a few isolated lines, thereby making it difficult to compare meaningfully the data on the different elements. This experiment measures transition probabilities for the bright halogen (F I, Cl I, Cl II, Br I) lines in the spectral region 4000–8700 Å. For the elements studied here, only the visible[1,2] and ultraviolet[3,4] Cl I, Cl II spectra have been investigated previously: For the F I, Br I, and the astrophysically important infrared Cl I spectra,[5] only theoretical predictions were heretofore available. This body of data can also be tested for possible systematic trends in the line[6] strengths of homologous atoms without recourse to theoretically estimated *A* values.

A gas-driven shock tube served as the thermal spectroscopic source. The thermodynamic state of the hot gas was determined by several independent methods. By these redundant state measurements and spectroscopic techniques which use plasma homogeneity to best advantage, absolute transition probabilities could be measured with accuracies of 20–40%.

II. EXPERIMENTAL PROCEDURE

The shock tube has a rectangular cross section of 6.8×9.3 cm^2 and the expansion chamber a length of 310 cm. Room-temperature hydrogen at 40–75 atm pressure drives the shock wave to the end of the tube, from which it is reflected, thereby heating the test gas twice by the shock process. The stationary gas sample at the end of the tube serves as our emitting source. Test gases were prepared in batches of 10 shots in a mixing manifold with several absolute pressure gauges. The test gas mixtures were allowed to equilibrate for several hours before being used. Thermodynamic conditions in the shock tube were deliberately varied to enhance weaker lines and as a precaution against systematic error.

Diagnostic instrumentation is shown schematically in Fig. 1. Temperatures were routinely measured to an accuracy of $\pm 1\frac{1}{2}\%$, pressure to $\pm 5\%$, and electron densities to $\pm 10\%$, using a combination of interrelated methods[7–14] based on local thermodynamic equilibrium (LTE) assumptions.

Four photoelectric spectrometers with a total of 18 recording channels viewed the hot gas in a single plane 2 cm upstream from the end wall of the shock tube. A 12-channel image dissector,[9] composed of 50-μ-thick microscope cover slides joined to fiber optics bundles, sampled 1-Å-wide slices of the H_β profile. Other photomultiplier channels recorded integrated intensities of optically thin lines and their adjacent continuum. The remaining photoelectric channels were used to record portions of H_α for emission and reversal temperature measurements. Absolute calibration of the photomultipliers at $\lambda \approx 6563$ Å was performed in both the conventional way using a regulated dc carbon arc[15] and by a new method which utilizes the *A* value and Stark profile of H_α as a fundamental intensity standard.[16] These

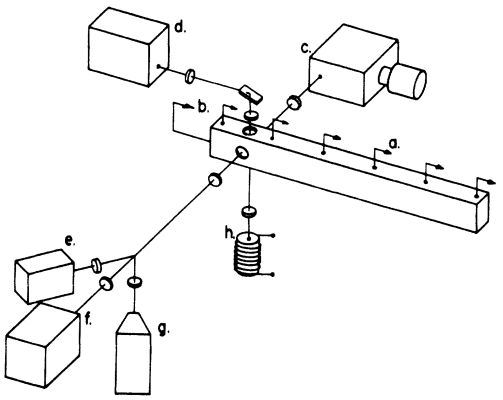

FIG. 1. Diagram of apparatus showing location of instrumentation: (a) ionization gaps for shock speed measurements; (b) quartz pressure transducers; (c) spectrograph with drum camera; (d) photoelectric monochrometer for reversal measurement; (e)–(g) photoelectric spectrographs; (h) flash lamp.

two calibrations agreed to within 5%. Photomultipliers at other wavelengths were calibrated using the carbon arc.[15] Line intensities observed with the photographic spectrograph were recorded with a high-speed revolving drum camera. With 70-mm film, approximately 1100 Å could be recorded for each shot with a typical time resolution of 10 μsec. Characteristic curves (photographic density versus log exposure) were determined using both a continuously variable Inconel neutral density wedge and a Kodak step filter. Spectral response of the emulsion was found using the carbon arc.[15] As a precaution against reciprocity failure, characteristic curves were determined with both the carbon arc and transient light sources. Computer codes,[14] which included optical depth corrections, converted digitized film densities to relative intensities. These relative intensities were then scaled to absolute intensities by comparing the photographic data with intensities from several absolutely calibrated photomulitpliers that simultaneously viewed the same plasma. No significant Eberhard (adjacency) effect, or reabsorption from the boundary layers, could be detected on the time-resolved spectra. Kodak 2475 and 103-0 films were used in the visible, while HSIR film was used in the infrared. Film developing and handling were done in a reproducible manner to minimize errors. Because a complete set of data for diagnostic state determinations and for transition probability measurements was made for each firing of the shock tube, reproducibility of test conditions or agreement with Hugoniot shock predictions was not necessary.

Data were analyzed by the method of thermally insensitive balancing (TIB) which minimizes systematic errors due to small uncertainties in the temperature of the emitting gas. Specific calculations and examples are given elsewhere,[7] but a brief review enables us to introduce a simple notation for describing the several types of A-value determinations and for analyzing the propagation of experimental error.

To specify the transition probability of a spectral line, we shall use the Einstein spontaneous emission probability A_{mn}. To determine experimentally A_{mn} for a transition from state m to state n, either an absolute or a relative measurement may be made. The absolute intensity of a spectral line is related to the population of the upper level N_m and the emission transition probability A_{mn} in a homogeneous optically thin light source of known composition of length l through the equation

$$I_{mn} = (hcl/4\pi\lambda) N_m A_{mn} \ . \qquad (1)$$

Measurement of I_{mn}, together with a knowledge of N_m obtained from state determinations (T, P) will determine an absolute emission value for A_{mn} (which we refer to as A^{emis}). A measurement of relative line intensities allows relative A values to be found through the equation

$$\frac{A_{mn}}{A_{pq}} = \frac{I_{mn}}{I_{pq}} \frac{N_p}{N_m} \frac{\lambda_{mn}}{\lambda_{pq}} \ . \qquad (2)$$

If A_{pq} is known, A_{mn} can be calculated. When Eq. (2) is applied to two lines of the same element in the stage of ionization, the factor (N_p/N_M) contains little thermal dependence. In a multicomponent plasma, Eq. (2) can also be used to find the absolute value of A_{mn}, often with higher accuracy than the standard emission method. In such a transpecies measurement, $A_{mn}/A_{pq} \approx N_p/N_m$ is generally a function of temperature and pressure. In some cases, however, a determination of A_{mn} from A_{mn}/A_{pq} (which we refer to as A^{rel}) has the *opposite* temperature dependence of A^{emis}. In such a situation, an appropriate combination of an emission and a relative measurement will have a lesser thermal dependence than either separately.[7]

Table I shows the TIB methods used in the present study to measure the transition probabilities, as well as the temperature ranges covered, and the chemicals added to the neon-carrier gas to produce the desired spectra.

III. RESULTS AND DISCUSSION

A. Fluorine

Temperatures in excess of 11 000 °K were required to give the fluorine lines photographically useful brightness. Excitation potentials of these lines are typically 15 times as great as mean thermal energies. Because emitter densities are critically dependent on temperature, the average of two relative intensity measurements was used to obtain an absolute transition probability which is relatively insensitive to thermal errors. The transition probability ($A_F^{\text{rel Ne}}$) measured relative to Ne λ 6678, was averaged with the transition probability ($A_F^{\text{rel}} H_\alpha$) measured relative to H_α (when H_α was optically thin) to give the thermally insensitive measurement shown in Fig. 2. A temperature uncertainty of ± 600 °K causes the average of these two measurements to be in error by only ± 3% even though upper-state number densities vary by a factor of 2 over the same range. The measured A values disclosed no apparent dependence on temperature, gas mixture, or type of film used. Scatter (5%) in the data and possible systematic errors, such as the 20% uncertainty[17] in the transition probability of Ne λ 6678, combine to give a probable error of ± 20% in the absolute A value. Experimental results are compared with results from the Coulomb approximation[17] in Table II. The present scale is lower by about 6% than that predicted by the Coulomb approximation.

Application of the J-file sum rule for the $3s$-$3p$ transition array of F I is illustrated in Table III.

TABLE I. Thermal balancing methods used in defining the transition probability, temperature ranges covered, and chemicals added to neon carrier gas to produce desired spectra.

Atom temperature range	Spectroscopic additives	Measurement method
Fluorine	$\frac{1}{4}\%\,CF_4+CH_4$	$A_F=\frac{1}{2}\frac{I_F\lambda_F}{N_F}\left(\frac{N_{H\alpha}A_{H\alpha}}{I_{H\alpha}\lambda_{H\alpha}}+\frac{N_nA_n}{I_n\lambda_n}\right)$
10 500–12 500 °K	$\frac{1}{4}\%\,CCl_2F_2+CH_4$	
Chlorine	$\frac{1}{3}$–$1\%\,CCl_4+CH_4$	$\lambda<7000$ Å
10 000–12 000 °K	$\frac{1}{3}$–$1\%\,CCl_2F_2+CH_4$	$A_{Cl\,I}=\frac{1}{2}\frac{I_{Cl}\lambda_{Cl}}{N_{Cl}}\left(\frac{N_{H\beta}A_{H\beta}}{I_{H\beta}\lambda_{H\beta}}+\frac{4\pi}{hcl}\right)$
		$\lambda>7000$ Å
		$A_{Cl\,I}=\frac{I_{Cl}\lambda_{Cl}}{N_{Cl}}\left(\frac{N_{H\alpha}A_{H\alpha}}{I_{H\alpha}\lambda_{H\alpha}}\right)$
		$A_{Cl\,I}=\frac{4\pi I_{Cl}\lambda_{Cl}}{N_{Cl}hcl}$
		$A_{Cl\,II}=\frac{I_{Cl}\lambda_{Cl}}{N_{Cl}}\left(\frac{N_{H\beta}A_{H\beta}}{I_{H\beta}\lambda_{H\beta}}\right)$
Bromine	$\frac{1}{2}$–$1\%\,CH_3Br$	$\lambda<700$ Å
10 000–12 000 °K		$A_{Br}=\frac{1}{2}\frac{I_{Br}\lambda_{Br}}{N_{Br}}\left(\frac{N_{H\beta}A_{H\beta}}{I_{H\beta}\lambda_{H\beta}}+\frac{4\pi}{hcl}\right)$
		$\lambda>7000$ Å
		$A_{Br}=\frac{I_{Br}\lambda_{Br}}{N_{Br}}\frac{4\pi}{hcl}$

The Coulomb approximation was used to calculate radial matrix elements $\sigma^2(r)$ for each line. The angular factors (S/σ^2) for each line in the transition array were normalized to the sum $\sum S/\sigma^2=54$. Lines too faint to be measured were estimated by assuming *LS* coupling within multiplets.

The *J*-file sums agree with the statistical weighting factors to within the estimated 20% experimental tolerance of the *A* values in all but three cases. The primary contribution to the sums in these three anomalous cases comes from lines all situated in the wavelength region 7300–7425 Å. Normally a serious error in the spectral response of films over so small a wavelength band could be completely ruled out. Although infrared films are particularly prone to a reciprocity failure, neither our calibration curves nor published film sensitivity curves indicated any rapid changes in sensitivity around 7375 Å.

LS coupling predictions for line strengths within multiplets agreed satisfactorily with experimental results.

B. Chlorine

Transition probabilities of the infrared chlorine lines ($4s$-$4p$ transition array) were measured by two different methods. The conventional emission (A_{Cl}^{emis}) measurement used an absolutely calibrated photomultiplier viewing the blended Cl λ 8376-Ne λ 8377 Å lines to set the absolute intensity scale for the simultaneously recorded photographic data. Optical depth corrections were applied to the integrated line profiles to reduce them to their optically thin limit. The second method based on Eq. (2) measured the transition probability of the Cl lines relative to the optically thin H_α λ 6563-Å line

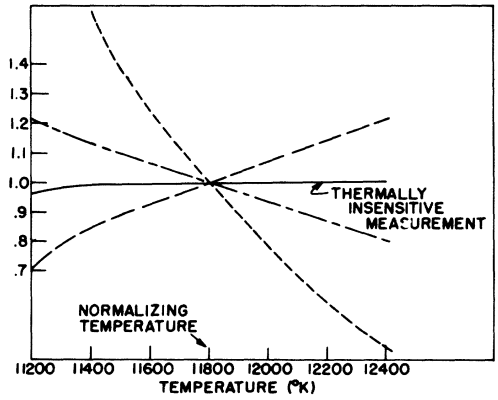

FIG. 2. Temperature dependence of excited-state number density N_F (F I λ 6856) dashed line, the ratios N (Ne λ 6678)/N (F λ 6856) dot-dashed line, $N(H_\alpha$ λ 6563)/N (F λ 6856) long-dashed line and the thermally insensitive measurement, solid line,

$$\frac{N(H_\alpha\ \lambda\ 6563)}{N(\mathrm{F\ I}\ \lambda\ 6856)}+\frac{N(\mathrm{Ne}\ \lambda\ 6678)}{N(\mathrm{F}\ \lambda\ 6856)}\,.$$

All curves are normalized to their values at $T=11\,800$ °K.

TABLE II. Transition probabilities for the $3s$-$3p$ transition array of F I.

Multiplet[a]	Transition	J_n-J_m	λ(Å)	A_{mn} (10^8 sec^{-1}) This experiment	A_{mn} (10^8 sec^{-1}) Coulomb approximation
1	$3s\,^4P$-$3p\,^4P^0$	$2\frac{1}{2}$-$2\frac{1}{2}$	7398.68	0.303 ± 20%	0.25
		$2\frac{1}{2}$-$1\frac{1}{2}$	7331.95	0.410 ± 20%	0.17
		$1\frac{1}{2}$-$\frac{1}{2}$	7425.64	0.351 ± 20%	0.30
		$1\frac{1}{2}$-$2\frac{1}{2}$	7552.24	0.079 ± 30%	0.10
		$\frac{1}{2}$-$1\frac{1}{2}$	7573.41	0.085 ± 30%	0.14
2	$3s\,^4P$-$3p\,^4D^0$	$2\frac{1}{2}$-$3\frac{1}{2}$	6856.02	0.400 ± 20%	0.45
		$1\frac{1}{2}$-$2\frac{1}{2}$	6902.46	0.292 ± 20%	0.31
		$\frac{1}{2}$-$1\frac{1}{2}$	6909.82	0.213 ± 20%	0.18
		$2\frac{1}{2}$-$2\frac{1}{2}$	6773.97	0.088 ± 30%	0.14
		$1\frac{1}{2}$-$1\frac{1}{2}$	6834.26	0.172 ± 20%	0.24
		$\frac{1}{2}$-$\frac{1}{2}$	6870.22	0.367 ± 20%	0.38
		$2\frac{1}{2}$-$1\frac{1}{2}$	6708.27	0.016 ± 30%	0.024
		$1\frac{1}{2}$-$\frac{1}{2}$	6795.52	0.038 ± 30%	0.077
3	$3s\,^4P$-$3p\,^4S^0$	$2\frac{1}{2}$-$1\frac{1}{2}$	6239.64	0.242 ± 20%	0.29
		$1\frac{1}{2}$-$1\frac{1}{2}$	6348.50	0.164 ± 20%	0.18
4	$3s\,^2P$-$3p\,^2D^0$	$1\frac{1}{2}$-$2\frac{1}{2}$	7754.70	0.313 ± 30%	0.35
		$\frac{1}{2}$-$1\frac{1}{2}$	7800.22	0.210 ± 30%	0.29
		$1\frac{1}{2}$-$1\frac{1}{2}$	7607.17	0.055 ± 50%	0.061
5	$3s\,^2P$-$3p\,^2S^0$	$1\frac{1}{2}$-$\frac{1}{2}$	7311.02	0.410 ± 30%	0.27
		$\frac{1}{2}$-$\frac{1}{2}$	7489.14	0.161 ± 50%	0.13
6	$3s\,^2P$-$3p\,^2P^0$	$1\frac{1}{2}$-$1\frac{1}{2}$	7037.45	0.248 ± 20%	0.38
		$\frac{1}{2}$-$\frac{1}{2}$	7127.88	0.331 ± 20%	0.30
		$1\frac{1}{2}$-$\frac{1}{2}$	6966.35	0.134 ± 50%	0.16
		$\frac{1}{2}$-$1\frac{1}{2}$	7202.37	0.081 ± 30%	0.072

[a]C. E. Moore, Natl. Bur. Std. (U. S.) Tech. News Bull. 36 (1959).

($A_{Cl}^{rel} H_\alpha$). The limited scan (1000 Å) of the 70-mm film prevented simultaneous application of both methods. The 15% difference between A_{Cl}^{emis} and $A_{Cl}^{rel} H_\alpha$ is larger than one would expect from random distribution and could be explained by either a systematic temperature error of ± 200 °K or by a relative intensity calibration error of 15% over the spectral range 6500–8500 Å. The possibility of an error in relative intensity calibration due to reciprocity failure is probably more likely. Al-

TABLE III. Experimental relative line strengths for fluorine $3s$-$3p$ transition array. Starred quantities (*) were found assuming LS coupling within multiplet.

Levels	^4P	^4D	^2S	^2P	^4S	^4P	^4D	^2P	^2D	^4P	^4D	^2D	^4D	Σ	g_u
^4P	0.39*	1.74	• • •	• • •	0.60*	1.25	2.04	• • •	• • •	• • •	• • •	• • •	• • •	6.02	2
^2P	• • •	• • •	0.86*	1.59	• • •	• • •	• • •	0.81	2.57	• • •	• • •	• • •	• • •	5.83	
^4P	2.10	0.18	• • •	• • •	1.30	0.53*	1.60	• • •	• • •	1.48	4.26	• • •	• • •	11.45	4
^2P	• • •	• • •	2.14	0.60*	• • •	• • •	• • •	2.98	0.64*	• • •	• • •	5.74	• • •	12.10	
^4P	• • •	• • •	• • •	• • •	1.80	2.36	0.14	• • •	• • •	5.45	1.20	• • •	7.65	18.60	6
Σ	2.49	1.92	3.00	2.19	3.70	4.14	3.78	3.79	3.21	6.93	5.46	5.74	7.65	54.00	
g_u		2				4					6		8		

though more data were taken using the emission method, the two methods are felt to be of comparable accuracy, and accordingly, A_{Cl}^{emis} and $A_{Cl}^{rel} H_\alpha$ are weighted equally. Estimated experimental error includes both the scatter in results and possible bias of temperature and photographic calibration. Transition probabilities of the infrared chlorine lines (up to the film cutoff at λ 8700 Å) are shown in Table IV. Our absolute scale agrees within 20% with the Coulomb approximation and *LS* coupling assumption for the strongest multiplets. Data for the strongest Cl I lines were not suitable for *A*-value determinations because radiative trapping was too severe under our normal shock tube conditions.

Cowan[18] has calculated intermediate-coupling line strengths for the 4*s*-4*p* transition array using *ab initio* calculations on the basis of Slater-Condon theory in the single configuration approach. Table V lists line strengths for this array as given by *LS* coupling, intermediate coupling, and experiment. All strengths are normalized to the presently measured value for Cl λ 8428 Å. Intermediate-coupling calculations yield much better agreement with experiment than do the *LS* predictions.

Absolute transition probabilities of the visible chlorine lines were determined simultaneously by both the emission method (A_{Cl}^{emis}) and by measurement relative to H_β ($A_{Cl}^{rel} H_\beta$). The average of these independent determinations is substantially less prone to error than either technique alone. Integrated visible line intensities for the A_{Cl}^{emis} measurements were obtained by fitting photographic intensity profiles to the absolute intensities simultaneously recorded by two photomultipliers viewing the continuum around 4600 Å. Best accuracy for the combined methods was achieved with Cl λ 4601 Å, where the *A* value 0.0424×10^8 sec^{-1} has a standard deviation of 4%. Probable error for the stronger lines is estimated to be ±20%. Results are shown in Table IV. Several of the weaker lines merged with carbon lines or with stronger chlorine lines. To unscramble tne blending, we used the relative intensities of Kiess.[19] This is felt to be a valid expedient because nearly all of the observed Cl I visible lines have the same excitation potential, making them relatively insensitive to source temperature or excitation mechanisms. Moreover, our data on unblended lines do agree well with Kiess's scale. Comparisons with *LS*- or intermediate-coupling predictions is not fruitful for visible lines because of cancellation in the radial matrix elements.

Present results generally agree with those of Foster.[1] Hey's[2] measurements, which were confined to a relatively few strong lines, also agree well when normalized to the present absolute scale.

The absolute transition probabilities of the ionized chlorine lines were measured relative to H_β. The high-excitation potentials of Cl II lines prevented optimal thermal balancing but the $A_{Cl\,II}^{rel} H_\beta$ data still have a much reduced thermal dependence as compared to absolute emission data. Table VI shows that measured transition probabilities agree closely with Coulomb approximations. One may suspect that this excellent agreement is somewhat fortuitous in view of the experimental and theoretical uncertainties. The latter are particularly large for multiplet (2), where transitions involve shell-equivalent electrons. Wherever comparison is possible, measurements of Foster[1] and Hey[2] satisfactorily overlap the present results.

C. Bromine

The first and second spectra of bromine were produced in a mixture of high-purity neon containing $\frac{1}{2}$–$1\frac{1}{2}$% methyl bromide (CH_3Br). Bromine data did not display the high degree of self-consistency which characterized our other experiments. Several discrepancies remain unexplained and tolerances for bromine are larger than for our other data. A systematic 10% difference between the electron density measured from the H_β profile and that calculated from measured pressures and temperatures is particularly puzzling. The fact that this disagreement was not encountered when a variety of other spectroscopic gases[8–10] was used suggests that methyl bromine may interact with the apparatus in some unknown way. Shocks in bromine and chlorine shots were made alternately and the self-consistency of chlorine data was excellent throughout all experiments. Methyl bromide should be stable against chemical reaction with the shock tube walls. Four mixtures, with nominal CH_3Br concentrations varying by more than a factor of 2, were used to test for possible chemical activity. There was no apparent correlation of measured *A* values with initial concentration of CH_3Br.

Uncertainty regarding the methyl-bromide concentration made it prudent to measure absolute Br I transition probabilities relative to H_β ($A_{Br}^{rel} H_\beta$), thus taking advantage of the stoichiometric fixed ratio of hydrogen to bromine. This measurement is sensitive to faulty temperature data but would only be slightly affected by errors in the concentration of methyl bromide. Barring systematic temperature errors, the other sources of repeatable errors are in photographic calibration, and small impurity concentrations of hydrogen from pump oil residue bouled off walls. Periodic checks using pure research-grade neon and argon shots showed effective residual atomic concentrations of hydrogen to be on the order of 0.1–0.2%.

Absolute transition probabilities for Br I are shown in Table VII. The line classification of Tech[20] is used. Although *LS* coupling is not appropriate for describing the bromine structure, the

TABLE IV. Measured Cl I transition probabilities and comparison with Coulomb approximation and other experiments.

Multiplet[a]	Transition	J_n-J_m	λ(Å)	Transition probability A_{mn} (10^8 sec^{-1}) This experiment	Foster (Ref. 1)	Hey (Ref. 2)	Coulomb approximation
2	$(^3D)4s\ ^4P$-$(^3D)4p\ ^4D$	$1\frac{1}{2}$-$2\frac{1}{2}$	8585.96	0.99 ± 30%			0.19
		$\frac{1}{2}$-$1\frac{1}{2}$	8575.25	0.114 ± 30%			0.129
		$2\frac{1}{2}$-$2\frac{1}{2}$	8212.00	0.055 ± 30%			0.101
		$1\frac{1}{2}$-$1\frac{1}{2}$	8333.29	0.089 ± 35%			0.16
		$\frac{1}{2}$-$\frac{1}{2}$	8428.25	0.190 ± 30%			0.270
		$1\frac{1}{2}$-$\frac{1}{2}$	8194.35	0.042 ± 35%			0.06
3	$4s\ ^1P$-$4p\ ^2D$	$2\frac{1}{2}$-$2\frac{1}{2}$	7878.22	0.0179 ± 30%			*LS*
		$1\frac{1}{2}$-$1\frac{1}{2}$	7997.80	0.0209 ± 30%			*LS*
		$1\frac{1}{2}$-$2\frac{1}{2}$	8221.73	0.056 ± 30%[b]			Forbidden
		$\frac{1}{2}$-$1\frac{1}{2}$	8220.40				
4	$4s\ ^1P$-$4p\ ^2P$	$2\frac{1}{2}$-$1\frac{1}{2}$	7414.10	0.047 ± 30%			*LS*
		$1\frac{1}{2}$-$1\frac{1}{2}$	7717.57	0.030 ± 30%			Forbidden
		$\frac{1}{2}$-$1\frac{1}{2}$	7924.62	0.021 ± 30%			
5	$4s\ ^1P$-$4p\ ^1S$	$2\frac{1}{2}$-$1\frac{1}{2}$	7256.63	0.152 ± 30%			0.226
		$1\frac{1}{2}$-$1\frac{1}{2}$	7547.06	0.120 ± 30%			0.140
		$\frac{1}{2}$-$1\frac{1}{2}$	7744.84	0.063 ± 30%			0.066
6	$4s\ ^1P$-$5p\ ^1P$	$2\frac{1}{2}$-$2\frac{1}{2}$	4438.48	0.0161 ± 20%	0.0112 ± 4%		
		$2\frac{1}{2}$-$1\frac{1}{2}$	4403.03	0.0083 ± 30%[c]	0.00648		Cancellation
		$\frac{1}{2}$-$1\frac{1}{2}$	4578.17	0.0018 ± 30%	0.00168 ± 15%		
7	$4s\ ^1P$-$5p\ ^1D$	$2\frac{1}{2}$-$3\frac{1}{2}$	4389.76	0.0144 ± 25%[d]	0.0129	0.0113	
		$1\frac{1}{2}$-$2\frac{1}{2}$	4475.31	0.0039 ± 20%	0.0047 ± 5%		
		$2\frac{1}{2}$-$2\frac{1}{2}$	4371.55	0.0004 ± 50%[e]	0.00144		Cancellation
		$1\frac{1}{2}$-$1\frac{1}{2}$	4379.90	0.0135 ± 20%	0.0103 ± 6%		
		$\frac{1}{2}$-$\frac{1}{2}$	4402.58	0.0067 ± 30%	0.00491		
8	$4s\ ^1P$-$5p\ ^2D$	$2\frac{1}{2}$-$2\frac{1}{2}$	4264.59	0.0017 ± 30%	0.00164 ± 12%		
		$\frac{1}{2}$-$1\frac{1}{2}$	4369.52	0.0075 ± 30%[e]	0.00639		Cancellation
		$1\frac{1}{2}$-$2\frac{1}{2}$	4363.30	0.0068 ± 30%	0.00649 ± 8%		
9	$4s\ ^1P$-$5p\ ^1S$	$2\frac{1}{2}$-$1\frac{1}{2}$	4226.44	0.0049 ± 30%	0.00606		
		$1\frac{1}{2}$-$1\frac{1}{2}$	4323.35	0.0109 ± 30%	0.0115 ± 4%		Cancellation
		$\frac{1}{2}$-$1\frac{1}{2}$	4387.55	0.0037 ± 50%[d]	0.00343		
13	$4s\ ^2P$-$4p\ ^2P$	$1\frac{1}{2}$-$\frac{1}{2}$	8550.46	0.0188 ± 50%			0.110
14	$4s\ ^2P$-$4p\ ^1S$	$1\frac{1}{2}$-$1\frac{1}{2}$	8686.28	0.0389 ± 30%			*LS* Forbidden
	$4s^2P$-$5p\ ^1D$	$1\frac{1}{2}$-$1\frac{1}{2}$	4740.74	0.0039 ± 30%	0.00453 ± 7%		*LS*
		$1\frac{1}{2}$-$\frac{1}{2}$	4691.53	0.0116 ± 30%	0.0108 ± 7%		Forbidden
	$4s\ ^2P$-$5p\ ^2D$	$1\frac{1}{2}$-$2\frac{1}{2}$	4721.24	0.0019 ± 30%	0.00223 ± 7%		Cancellation
		$1\frac{1}{2}$-$1\frac{1}{2}$	4654.05	0.0051 ± 30%	0.00467 ± 9%		
	$4s\ ^2P$-$5p\ ^2S$	$1\frac{1}{2}$-$\frac{1}{2}$	4677.76	0.0056 ± 30%	0.0052 ± 18%		Cancellation
	$4s\ ^2P$-$5p\ ^4S$	$1\frac{1}{2}$-$1\frac{1}{2}$	4674.40	0.0021 ± 50%	0.00181		Cancellation
15	$4s\ ^2P$-$5p\ ^2P$	$1\frac{1}{2}$-$1\frac{1}{2}$	4526.20	0.0513 ± 20%	0.0407 ± 2%	0.0333	
		$\frac{1}{2}$-$\frac{1}{2}$	4601.00	0.0424 ± 15%	0.0421 ± 3%	0.0323	
		$1\frac{1}{2}$-$\frac{1}{2}$	4469.37	0.0205 ± 30%	0.0122 ± 7%		Cancellation
		$\frac{1}{2}$-$1\frac{1}{2}$	4661.22	0.0121 ± 20%	0.00846 ± 5%		
	$4s\ ^2P$-$(^1D)\ 5p\ ^2D$	$1\frac{1}{2}$-$1\frac{1}{2}$	4491.05	0.0051 ± 30%	0.00453		Cancellation
		$\frac{1}{2}$-$1\frac{1}{2}$	4623.96	0.0046 ± 30%	0.00438 ± 7%		
	$4s\ ^2P$-$(^1D)\ 5p\ ^2P$	$1\frac{1}{2}$-$1\frac{1}{2}$	4976.62	0.0030 ± 50%	0.00403 ± 18%		Cancellation
	$4s\ ^2D$-$(^1D)4p\ ^2D$	$2\frac{1}{2}$-$2\frac{1}{2}$	8086.67				
		$1\frac{1}{2}$-$2\frac{1}{2}$	8087.67	0.284 ± 30%[b]			
		$1\frac{1}{2}$-$1\frac{1}{2}$	8085.54				
		$2\frac{1}{2}$-$1\frac{1}{2}$	8084.48				
	$(^3D)4p\ ^4P$-$(^3D)4d\ ^4D$	$2\frac{1}{2}$-$3\frac{1}{2}$	7821.35	0.098 ± 35%			
		$1\frac{1}{2}$-$2\frac{1}{2}$	7899.28	0.051 ± 35%			
		$2\frac{1}{2}$-$2\frac{1}{2}$	7769.18	0.060 ± 35%			
		$1\frac{1}{2}$-$1\frac{1}{2}$	7830.76	0.097 ± 35%			
		$\frac{1}{2}$-$\frac{1}{2}$	7915.09	0.044 ± 35%			
		$1\frac{1}{2}$-$\frac{1}{2}$	7771.10	0.030 ± 35%			
	$4p\ ^4D$-$4d\ ^4F$	$2\frac{1}{2}$-$3\frac{1}{2}$	7935.00	0.0387 ± 35%			

[a] C. E. Moore, Natl. Bur. Std. (U. S.) Tech. News Bull. 36 (1959).

[b] Blended lines.

[c] Relative intensity scale of Kiess to separate blend of Cl λ 4402.58, Cl λ 4403.03.

[d] Relative intensity scale of Kiess to separate blend of Cl λ 4389.76, Cl λ 4387.55, and Cl λ 4390.38.

[e] Blend Cl λ 4371.55, Cl λ 4369.52, and Cl λ 4371.33. Corrected using carbon transition probability from Ref. 9 and Kiess's relative values.

TABLE V. Comparison of measured line strengths to strengths predicted from intermediate coupling and *LS* coupling for the $4s$-$4p$ transition array of Cl I.

Multiplet[a]	Transition	J_i-J_k	λ(Å)	This experiment	Intermediate coupling[b]	*LS* coupling
2	$4s\,^4P$-$4p\,^4D$	$\frac{1}{2}$-$\frac{1}{2}$	8428.25	11.27[c]	11.27[c]	11.27[c]
		$1\frac{1}{2}$-$2\frac{1}{2}$	8585.96	18.72	26.10	28.45
		$\frac{1}{2}$-$1\frac{1}{2}$	8575.25	14.18	11.63	11.27
		$2\frac{1}{2}$-$2\frac{1}{2}$	8212.00	9.10	4.28	12.17
		$1\frac{1}{2}$-$1\frac{1}{2}$	8333.29	10.14	11.39	14.49
		$1\frac{1}{2}$-$\frac{1}{2}$	8149.35	2.27	1.14	2.28
3	$4s\,^4P$-$4p\,^2D$	$2\frac{1}{2}$-$2\frac{1}{2}$	7878.22	2.60	1.01	
		$1\frac{1}{2}$-$1\frac{1}{2}$	7997.80	2.11	0.33	Forbidden
		$1\frac{1}{2}$-$2\frac{1}{2}$	8221.73	15.40[d]	6.10	
		$\frac{1}{2}$-$1\frac{1}{2}$	8220.40		1.80	
4	$4s\,^4P$-$4p\,^2P$	$2\frac{1}{2}$-$1\frac{1}{2}$	7414.10	3.76	1.34	
		$1\frac{1}{2}$-$1\frac{1}{2}$	7717.56	2.72	1.54	Forbidden
		$\frac{1}{2}$-$1\frac{1}{2}$	7924.62	2.05	0.656	
5	$4s\,^4P$-$4p\,^4P$	$2\frac{1}{2}$-$1\frac{1}{2}$	7256.63	11.51	7.72	13.50
		$1\frac{1}{2}$-$1\frac{1}{2}$	7547.06	10.22	7.61	9.02
		$\frac{1}{2}$-$1\frac{1}{2}$	7744.84	5.86	5.69	4.52
13	$4s\,^2P$-$4p\,^2P$	$1\frac{1}{2}$-$\frac{1}{2}$	8550.46	1.10	1.17	4.51
14	$4s^2P$-$4p\,^4S$	$1\frac{1}{2}$-$1\frac{1}{2}$	8686.28	5.04	2.30	Forbidden

[a]C. E. Moore, Natl. Bur. Std. (U. S.) Tech. News Bull. 36 (1959).
[b]Reference 20.
[c]All data normalized to the experimental line strength for 8428-Å line.
[d]Blended lines.

usual *LS* notation has been adopted. The ± 30% tolerance takes into account possible errors in the initial bromine concentrations, temperature determinations, and photographic calibration. Scatter is responsible for less than 15% of the uncertainty in any absolute A values.

The absolute transition probabilities of infrared bromine lines were measured by the emission

TABLE VI. Measured Cl II transition probabilities and comparison with literature values and Coulomb approximation.

				Transition probabilities $A_{mn}(10^8\ \mathrm{sec}^{-1})$			
Multiplet[a]	Transition	J_n-J_m	λ (Å)	This experiment	Foster (Ref. 1)	Hey (Ref. 2)	Coulomb approximation
1	$4s\,^5S$-$4p\,^5P$	2-3	4794.54	1.04 ± 25%	1.47	1.2	1.01
		2-2	4810.06	0.99 ± 25%	1.39	···	1.00
		2-1	4819.46	1.00 ± 25%	1.32	···	1.00
2	$3d\,^5D$-$4p\,^5D$	4-3	5423.25	0.18 ± 50%[b]	···	···	0.196
		3-2	5443.42	0.15 ± 50%[b]			0.135
		2-1	5456.27	0.084 ± 50%[b]			0.084
		3-3	5423.52	0.037 ± 50%[b]			0.048
		2-2	5444.25	0.095 ± 50%[b]			0.084
		1-1	5457.02	0.108 ± 50%[b]			0.108
		2-3	5424.36	0.005 ± 50%[b]			0.007
		1-2	5444.29	0.024 ± 50%[b]			0.022
		0-1	5457.47	0.048 ± 50%[b]			0.048
3	$4s\,^3S$-$4p\,^3P$	1-4[c]	5218[c]	0.86 ± 25%	0.58	···	0.875
17	$4s\,^3D$-$4p\,^3F$	3-4	4896.77	0.80 ± 50%	···	···	0.97
19	$4s\,^3D$-$4p\,^3P$	3-2	4343.62	0.50 ± 50%	···	···	1.2
28	$4s\,^1D$-$4p\,^1F$	2-3	5392.12	1.0 ± 50%	···	···	0.77

[a]C. E. Moore, Natl. Bur. Std. (U. S.) Tech. News Bull. 36 (1959).
[b]*LS* coupling used to separate components of blended lines.
[c]Multiplet values listed.

TABLE VII. Measured Br I transition probabilities.

Transition	J_n-J_m	λ(Å)	Transition probability A_{mn} (10^8 sec^{-1})
$(^3P_2)5s\ ^4P$-$(^3P_2)5p\ ^4P$	$2\frac{1}{2}$-$1\frac{1}{2}$	8638.66	0.096 9 ± 35%
$5s\ ^4P$-$5p\ ^4D$	$2\frac{1}{2}$-$3\frac{1}{2}$	8272.44[a]	0.117 ± 50%
	$2\frac{1}{2}$-$2\frac{1}{2}$	8154.00	0.009 6 ± 50%
	$1\frac{1}{2}$-$1\frac{1}{2}$	8446.55	0.117 ± 35%
	$2\frac{1}{2}$-$1\frac{1}{2}$	7512.96	0.116 ± 35%
$(^3P_2)5s\ ^4P$-$(^3P_1)5p\ ^4S$	$1\frac{1}{2}$-$1\frac{1}{2}$	7005.19	0.123 ± 50%
$5s\ ^2P$-$5p\ ^2P$	$2\frac{1}{2}$-$2\frac{1}{2}$	6631.62	0.139 ± 50%
	$1\frac{1}{2}$-$2\frac{1}{2}$	7348.51	0.119 ± 35%
$(^3P_1)5s\ ^4P$-$(^3P_1)5p\ ^4D$	$\frac{1}{2}$-$\frac{1}{2}$	8343.70	0.219 ± 35%
$5s\ ^4P$-$5p\ ^4S$	$\frac{1}{2}$-$1\frac{1}{2}$	8131.52	0.037 9 ± 35%
$5s\ ^2P$-$5p\ ^2S$	$1\frac{1}{2}$-$1\frac{1}{2}$	8334.70[b]	0.146 ± 50%
$(^3P_1)5s\ ^2P$-$(^3P_0)5p\ ^2P$	$1\frac{1}{2}$-$1\frac{1}{2}$	7989.94	0.029 6 ± 50%
$5s\ ^4P$-$5p\ ^2P$	$\frac{1}{2}$-$1\frac{1}{2}$	7803.02	0.053 3 ± 35%
$(^3P_2)5s\ ^4P$-$(^3P_2)6p\ ^4P$	$2\frac{1}{2}$-$2\frac{1}{2}$	4525.59	0.007 21 ± 25%
	$2\frac{1}{2}$-$1\frac{1}{2}$	4513.44	0.002 8 ± 25%
$5s\ ^4P$-$6p\ ^4D$	$2\frac{1}{2}$-$3\frac{1}{2}$	4477.72	0.012 7 ± 25%
	$2\frac{1}{2}$-$1\frac{1}{2}$	4441.74	0.007 47 ± 25%
$(^3P_1)5s\ ^2P$-$(^3P_2)6p\ ^4P$	$1\frac{1}{2}$-$\frac{1}{2}$	5370.34	0.000 24 ± 50%
$5s\ ^2P$-$6p\ ^4P$	$1\frac{1}{2}$-$2\frac{1}{2}$	5364.19	0.000 14 ± 50%
$5s\ ^4P$-$6p\ ^4P$	$\frac{1}{2}$-$1\frac{1}{2}$	5345.42	0.007 61 ± 25%
$5s\ ^4P$-$6p\ ^4D$	$\frac{1}{2}$-$1\frac{1}{2}$	5245.12	0.003 14 ± 25%
$(^3P_2)5s\ ^4P$-$(^1D_2)5p\ ^2P$	$1\frac{1}{2}$-$1\frac{1}{2}$	4472.61	0.009 3 ± 25%
	$1\frac{1}{2}$-$\frac{1}{2}$	4425.14	0.004 2 ± 25%
$(^3P_1)5s\ ^2P$-$(^1D_2)5p\ ^2P$	$1\frac{1}{2}$-$1\frac{1}{2}$	4979.76	0.002 61 ± 25%
$(^3P_0)5s\ ^2P$-$(^1D_2)5p\ ^2P$	$1\frac{1}{2}$-$1\frac{1}{2}$	5395.53	0.010 8 ± 50%
$(^1D_2)5s\ ^2D$-$(^1D_2)5p\ ^2D$	$2\frac{1}{2}$-$2\frac{1}{2}$	7938.68	0.190 ± 35%
	$1\frac{1}{2}$-$1\frac{1}{2}$	7978.50	0.130 ± 35%
$(^3P_1)5s\ ^4P$-$(^3P_1)6p\ ^4D$	$\frac{1}{2}$-$\frac{1}{2}$	4490.42	0.007 8 ± 50%
$5s\ ^2P$-$6p\ ^4S$	$1\frac{1}{2}$-$1\frac{1}{2}$	4575.74	0.015 6 ± 25%
$5s\ ^2P$-$6p\ ^2D$	$1\frac{1}{2}$-$2\frac{1}{2}$	4614.58	0.005 39 ± 25%
$(^3P_1)5s\ ^4P$-$(^3P_2)7p\ ^4D$	$\frac{1}{2}$-$1\frac{1}{2}$	4365.14	0.007 5 ± 25%

[a]Self-absorption.
[b]Correction for C 8335 Å.

(A^{emis}_{Br}) method. Absolute photometric calibrations of the film at this wavelength, using techniques already described, are felt to be reliable to ±15%. Estimated tolerances (± 35%) are relatively large because possible errors in bromine concentration carry over directly into the A^{emis}_{Br} data. Corrections for self-absorption are smaller for the bromine data than for chlorine.

Pronounced intermediate coupling,[20] complicated by configuration interactions, makes it difficult to theoretically predict line strengths of neutral bromine.

IV. CONCLUSIONS

Transition probabilities of visible and near-infrared halogen lines have been measured with identical equipment and techniques. To interrelate the data for the various spectra more closely, two or more of the elements fluorine, chlorine, and bromine were frequently studied simultaneously in the shock tube. Investigations[8,9] of other elements such as carbon and silicon will further correlate the halogen data with other accurate measurements. This consistent experimental program allows us to meaningfully examine data on homologous atoms for possible systematic trends in either absolute or relative gf values. It has been suggested [6,17] that multiplet f values[17] in dominant transition arrays remain approximately constant throughout a family of atoms having the same number of valence electrons. The f values of the 4_P-4_S multiplet of the $np^4(n+1)s - np^4(n+1)p$ transition array in fluorine, chlorine, and bromine shown in Fig. 3 do remain

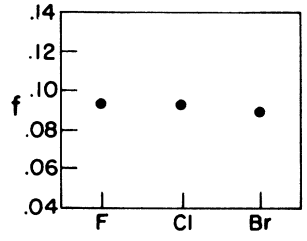

FIG. 3. Multiplet f values for the ^4P-^4S multiplet of the $np^4\ (n+1)s - n^4(n+1)p$ transition array of F I, Cl I, Br I.

constant. It is unknown whether this trend is representative or fortuitous since the spectral range of our apparatus unfortunately did not permit study of the complete transition array.

Coulomb approximation and experimental A values generally agree within 30% for the cases where the radial integrals do not approach cancellation. Relative line strengths within the $3s$-$3p$ transition array of neutral fluorine are described reasonably well by LS coupling. However, for the other neutral halogens, LS coupling is clearly not a useful approximation.

ACKNOWLEDGMENTS

The authors would like to express their thanks to E. Grossenbacher, G. Monahan, R. Roig, W. Roig, P. Debeilus, and E. Pocock for their assistance in this work. We are also indebted to R. Cowan for performing the intermediate-coupling calculations. Computer time was provided by the Computer Science Center of the University of Maryland from National Aeronautics and Space Administration Grant No. NsG 398.

---

*Work supported in part by NASA Grant Nos. NsG-359, NGR 21-002-007, NSF Grant No. GP 8325, and contributions from the Regents of the University of Maryland.

†Present address: Physics Department, University of Texas at Austin, Austin, Tex. 78712.

[1]E. W. Foster, Proc. Phys. Soc. (London) 80, 882 (1962).

[2]P. Hey, Z. Physik 157, 79 (1959).

[3]G. M. Lawrence, Astrophys. J. 148, 261 (1967).

[4]W. Hofmann, Z. Naturforsch. 22a, 2097 (1967).

[5]D. L. Lambert and E. A. Mallia, Solar Phys. 5, 181 (1968).

[6]W. L. Wiese and A. W. Weiss, Phys. Rev. 175, 50 (1968).

[7]M. H. Miller, J. Quant. Spectry. Radiative Transfer 9, 1251 (1969).

[8]R. D. Bengtson, University of Maryland Technical Note No. BN-599, 1968 (unpublished).

[9]M. H. Miller, University of Maryland Technical Note No. BN-550, 1968 (unpublished).

[10]M. H. Miller and R. D. Bengtson, Phys. Rev. A 1, 983 (1970).

[11]R. D. Bengtson, M. H. Miller, D. W. Koopman, and T. D. Wilkerson, Phys. Fluids 13, 372 (1970).

[12]R. D. Bengtson and M. H. Miller, J. Opt. Soc. Am. 60, 1093 (1970).

[13]D. W. Koopman, University of Maryland Technical Note No. BN-481, 1966 (unpublished).

[14]R. A. Bell, R. D. Bengtson, D. R. Branch, D. M. Gottlieb, and R. A. Roig, University of Maryland Technical Note No. BN-572, 1968 (unpublished).

[15]A. T. Hattenburg, Appl. Opt. 6, 95 (1967).

[16]M. H. Miller and R. D. Bengtson, J. Quant. Spectry. Radiative Transfer 9, 1573 (1969).

[17]W. L. Wiese, M. W. Smith, and B. M. Glennon, Natl. Bur. Std. (U. S.) 4, 1 (1966); W. L. Wiese, M. W. Smith, and B. M. Miles, *ibid.* 2, 22 (1969).

[18]R. D. Cowan (private communication); J. Opt. Soc. Am. 58, 808 (1968).

[19]C. C. Kiess, Natl. Bur. Std. J. Res., 10, 827 (1933).

[20]J. L. Tech, J. Res. Natl. Bur. Std. (U. S.) 67A, 505 (1963).